

Chapter 4

Development of Amorphous Silicon Alloy Thin Film Light Emitting Diode Having a-SiC:H as a Luminescent Layer

4.1 Introduction

In this work, a novel visible-light a-SiN:H thin film LED (TFLED) was developed and the details have been described in chapter 3. The brightness of the a-SiN:H TFLEDs was the level of 0.7-0.8 cd/m². It is necessary to explore new materials for brighter amorphous TFLEDs. In this chapter, the results on the fabrication and investigation of basic properties of amorphous TFLED having a-SiC:H as a luminescent layer are described.

Hydrogenated amorphous silicon carbide (a-SiC:H) films are widely prepared by a glow discharge plasma CVD method from various gas combinations, such as silane-ethylane [1-5], silane-methane [6-7], tetramethylsilane [8] and trimethylsilane [9]. The alloy composition can be changed over a wide range by controlling the mixing ratio of gases and deposition parameters. Tawada et al. succeeded for the first time in doping a-SiC:H and developed high efficiency a-SiC:H/a-Si:H heterojunction solar cells [6]. Since then the application field of a-SiC:H has been expanding into various optoelectronic devices, such as a-SiC:H/c-Si heterojunction bipolar transistor, linear imaging sensor, CCD imager and photoreceptor, visible-light thin film LED [5,10].

In this chapter, a-SiC:H p-i-n junction TFLED is fabricated. The results of a systematic study on the fabrication and characterizations including photoluminescence of a-SiC:H are presented. The brightness of the a-SiC:H TFLED is 1-2 cd/m² which is better than the case of a-SiN:H TFLED and the emission is bright enough to be observed in a normal room. It is revealed that the a-SiC:H TFLED can be operated by a pulse current mode with the modulation frequency as high as 500 kHz. The yellow and orange color a-SiC:H TFLED displays with various emitting patterns and areas of several cm² are demonstrated.

4.2 Preparation of a-SiC:H Films

Undoped a-SiC:H was prepared by rf (13.56 MHz) glow discharge plasma CVD method as mentioned in chapter 2. SiH₄ (diluted in H₂ to 10 %) and C₂H₄ (diluted in H₂ to 10%) were used as source gases. The total pressure during growth was 1 torr. The substrate temperature was 190 °C. The typical preparation conditions for undoped a-SiC:H are summarized in Table 4.1. The deposition rate of the a-SiC:H is about 3-5 Å/sec.

Table 4.1 Typical preparation conditions for undoped a-SiC:H

RF Power	3 Watt
Substrate Temperature	190 °C
Gas Pressure	1 Torr
Gas Fraction	$x = C_2H_4 / (SiH_4 + C_2H_4)$
Film Thickness	1.0 - 1.5 micron

4.3 Study of Structural Properties of a-SiC:H Films by IR Absorption and ESR

The structural properties of undoped a-SiC:H were investigated by using infrared absorption and ESR techniques. It was found that hydrogen is bonded with both silicon and carbon. The hydrogen content in the a-SiC:H film prepared in the work was estimated to be about 20-30% by atomic number.

The ESR spectra were taken by the Jeol model JES-RE2X ESR spectrometer. The spin density was determined by calibration with the standard sample; DPPH (1, 1-dyphenil-2-pyrylhydrazil). Figure 4.1 shows ESR spin density of undoped a-SiC:H as a function of the carbon gas fraction $x = C_2H_4 / (SiH_4 + C_2H_4)$. The spin density increases from 10^{16} 1/cm³ to about 10^{18} 1/cm³ when the carbon gas fraction x increases from 0 to 0.8, and at the same time the g-value decreases from 2.0055 to 2.0030. The g-value decreases with increasing the carbon gas fraction because of the interaction of Si dangling bond with surrounding C atoms.

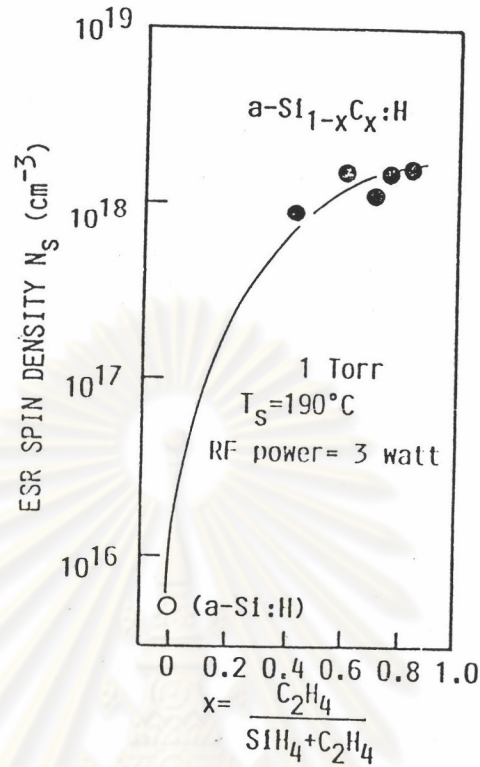


Figure 4.1 ESR spin density of undoped a-SiC:H as a function of carbon gas fraction $x = C_2H_4/(SiH_4+C_2H_4)$.

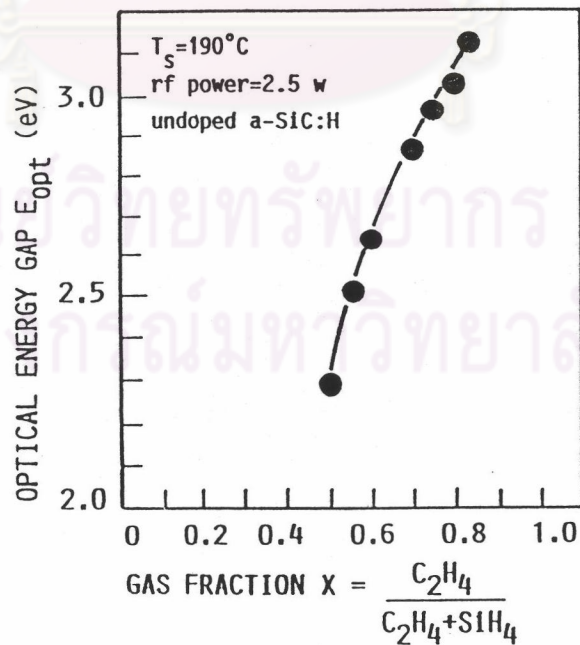


Figure 4.2 Relationship between the optical energy gap of undoped a-SiC:H and carbon gas fraction $x = C_2H_4/(SiH_4+C_2H_4)$.

4.4 Optical Properties of a-SiC:H Films

4.4.1 Optical Absorption Edge of a-SiC:H Films

Figure 4.2 shows the relation between the optical energy gap of undoped a-SiC:H and the carbon gas fraction $x = C_2H_4/(SiH_4+C_2H_4)$. Here, the optical energy gap of a-SiC:H was determined from the Tauc's plot of $(\alpha\nu)^{1/2}$ vs $(h\nu)$. The optical energy gap of undoped a-SiC:H increases monotonically as the carbon content increases from that of a-Si:H of about 1.75 eV to 3.2 eV. It is confirmed in this experiment that large optical energy gap a-SiC:H can be produced. As will be shown in the next section, the a-SiC:H with the optical energy gap larger than about 2.5 eV will be used as the i-layer in the p-i-n junction TFLED.

4.4.2 Photoluminescence (PL) of a-SiC:H Films

Photoluminescence is a technique widely used for studying localized states within the band gap of a semiconductor. The technique is therefore particularly applicable to amorphous semiconductors, since much of the interest in these materials relate to the localized states introduced by intrinsic disorder or by specific defects. In early studies of amorphous silicon, photoluminescence was undetectable, because the density of defects was so large that nonradiative recombination was dominant. Hydrogen by glow discharge or by reactive sputtering reduced the defect density, and it was quickly found that this material had strong luminescence [11]. Since then, many studies of the emission have been reported [12-15], and from these, a clear picture of the various low-temperature recombination processes has emerged, including the different nonradiative processes. The photoluminescent spectra of glow-discharge produced a-Si:H were generally observed at low temperature and showed a single intense emission band near 1.3 - 1.4 eV with a full width at half maximum of around 0.28 eV. When the temperature is increased, the luminescent intensity decreases, the peak moves to lower energy, and eventually a second peak near 0.90 eV was observed. The interest in the photoluminescent properties of a-Si:H was mostly paid to the study of the nature of localized states, rather than to the

exploration of a light emitting device, because the emission was almost in the infrared region.

Our interest in this work is to explore a visible light emitting diode, so we need a wider band gap material. One of the candidates as wide gap amorphous semiconductors is a-SiC:H. The a-SiC:H was first prepared by Anderson and Spear [1]. Engeman et al. first reported that a-SiC:H shows a visible photoluminescence [2]. Since then many authors reported on the photoluminescent properties of a-SiC:H [4, 7,9,15]. One of the most excellent reviews has been presented in the paper reported by Sussman [4]. However, most of them concerned with photoluminescence were measured at low temperature.

In this section, the photoluminescent properties at room temperature of undoped a-SiC:H having a wide range of optical energy gap from 2.0 eV to more than 3.2 eV are presented.

Undoped a-SiC:H was prepared by rf plasma CVD method from mixture of silane and carbon source gases, such as methane or ethylene. The optical energy gap was varied by changing the carbon gas fraction. Photoluminescent measurements were carried out at room temperature using a 3250 Å He-Cd laser as an excitation source.

Figure 4.3 shows the room temperature PL spectra of undoped a-SiC:H prepared from a mixture of silane and ethylene. The parameter in the figure is the optical energy gap of a-SiC:H. The PL spectra show a single broad band. The emission color of the PL can be controlled from red to green by adjusting the optical energy gap from 2.25 eV to about 3.5 eV. The spectra shift toward higher energies with increasing the optical energy gap. At the same time the spectra tend to become broader, implying increased compositional fluctuation or an enhanced electron-phonon interaction.

Figure 4.4 shows the dependences of the PL peak energy and optical energy gap of a-SiC:H on the carbon gas fraction $x = C_2H_4/(SiH_4+C_2H_4)$. The PL peak energy (E_{PL}) as well as the optical energy gap increase as the carbon gas fraction increases. It should be noted that the PL peak energy usually shows a stoke shift lying

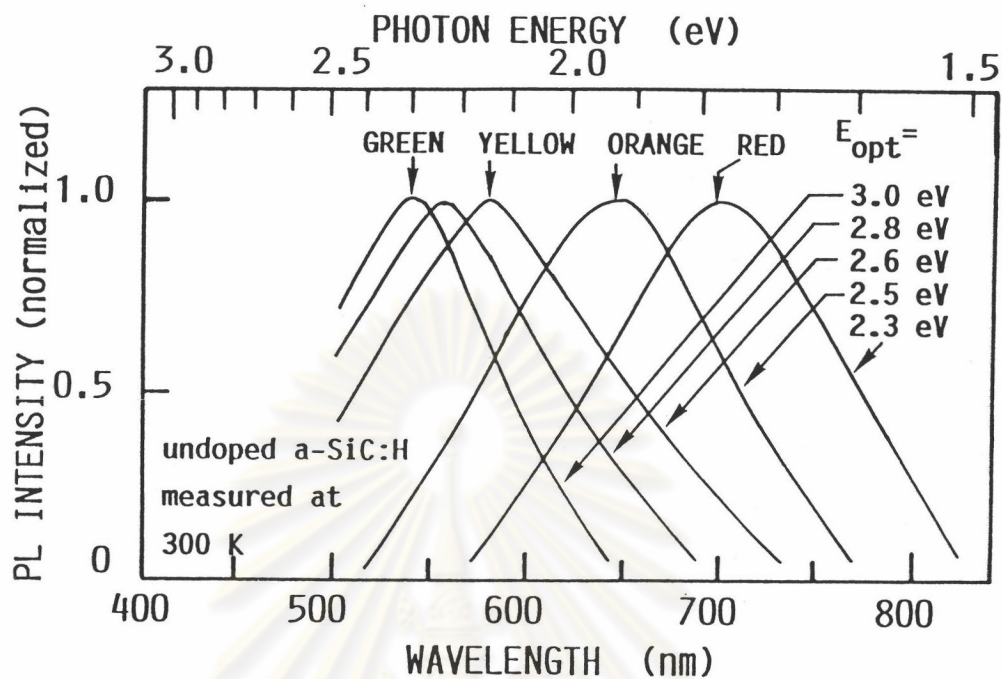


Figure 4.3 Room temperature PL spectra of undoped a-SiC:H prepared from mixtures of silane and ethylene.

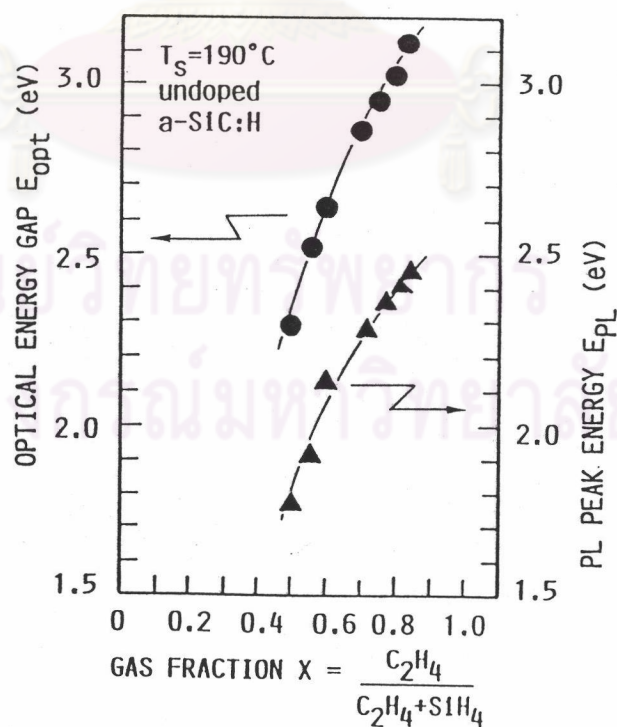


Figure 4.4 Dependences of the PL peak energy and the optical energy gap of a-SiC:H on the carbon gas fraction $x = \frac{C_2H_4}{C_2H_4 + SiH_4}$.

at an energy lower than its optical energy gap. The Stokes shift might be caused by the distortion of lattices in part and/or by the relaxation of carriers down into deep states before recombinations take place. It is likely that as the optical gap increases, the value of $E_{\text{opt}} - E_{\text{PL}}$ and the full width of PL spectrum become larger. This might imply that as the carbon content increases, the distribution of the radiative recombination centers becomes broader and deeper within the gap.

It is found in Fig. 4.4 that the a-SiC:H that exhibits visible PL should have the optical energy larger than about 2.5 eV.

4.5 Structure and Fabrication of Thin Film Light Emitting Diode Having a-SiC:H as a Luminescent Layer

a-SiC:H TFLED developed in this work has a structure of glass/ITO/p-a-SiC:H/i-a-SiC:H/n-a-SiC:H/Al [17-20]. Figure 4.5 shows a schematic illustration of the structure of the a-SiC:H TFLED. The cell area was 0.33 - 5 cm². In this type of TFLED, p- and n-layers act as injectors of holes and electrons, respectively, into the luminescent active i-layer. The thicknesses of the p-i-n layers are 150 Å, 500 Å and 500 Å, respectively. The optical energy gap of the luminescent i-layer necessary for visible light was varied in the range from 2.5 eV to 3.1 eV. The EL intensity also strongly depends on the thickness and optical energy gap of the i-layer, and the details of these dependences will be described in the following sections.

Figure 4.6 shows schematic band diagrams of a-SiC:H p-i-n junctions in (a) thermal equilibrium and in (b) forward bias conditions. The injection electroluminescence can be observed when the diode is positively biased. In order to obtain a visible luminescence, the optical energy gap of the i-layer has to be larger than about 2.3 eV, as deduced from the results of the photoluminescent data in the previous section. While the optical energy gaps of p- and n- a-SiC:H layers should be chosen, at most, around 2.0 eV to ensure the effective valency controllability to p- and n-type semiconductors, respectively. Therefore, holes and electrons are injected into the i-layer by tunneling effects through the notch barriers at the p/i and i/n interfaces, respectively.

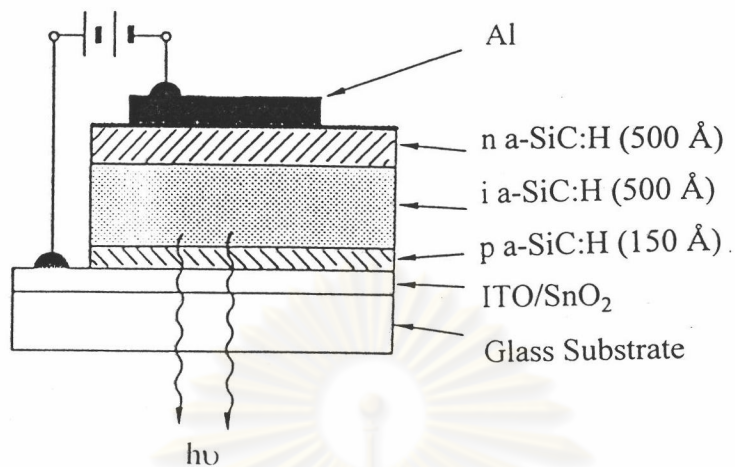
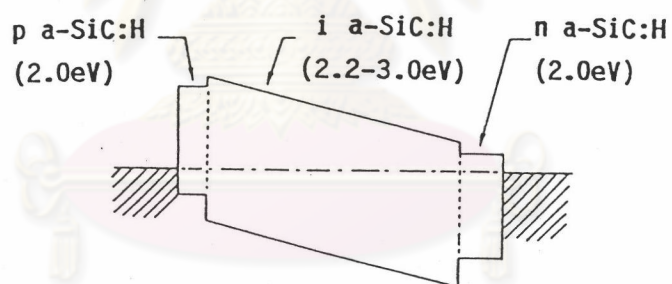
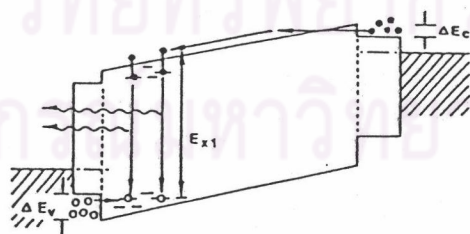


Figure 4.5 Schematic illustration of the structure of the a-SiC:H TFLED.



(a) ZERO BIAS



(b) FORWARD BIAS

Figure 4.6 Schematic band diagrams of a-SiC:H p-i-n junctions in (a) thermal equilibrium and (b) forward bias conditions.

The p-i-n a-SiC:H layers were deposited by the glow discharge plasma CVD system as mentioned in chapter 2. The typical preparation conditions for the p-i-n a-SiC:H layers are shown in Table 4.2

Table 4.2 Typical preparation conditions of a-SiC:H TFLED

Power Source	C-Coupling, 13.56 MHz
RF Power	4 Watt
Substrate Temperature	190 °C
Total Gas Pressure	1.0 Torr.
p-type a-SiC:H	SiH ₄ /CH ₄ /B ₂ H ₆ = 1.5/3.5/0.03
i-type a-SiC:H	SiH ₄ /C ₂ H ₄ = 1/3
n-type a-SiC:H	SiH ₄ /CH ₄ /PH ₃ = 1.5/3.5/0.03
Cell Area	0.033 - 5 cm ²

4.6 Basic Characteristics of a-SiC:H TFLED

The a-SiC:H TFLED fabricated in this work has a structure of glass/ITO/p-a-SiC:H/i-a-SiC:H/n-a-SiC:H junctions. In this section 4.6, basic characteristics of the a-SiC:H TFLED including carrier injection mechanism, EL spectra, dependence of brightness on current and frequency-modulation will be described.

4.6.1 Carrier Injection Mechanism in a-SiC:H TFLED

Figure 4.7 shows plots of the I-V curves of a-SiC:H TFLEDs measured at room temperature. The parameter in the figure is the optical energy gap of the i-layer, i.e., 2.60, 2.85 and 3.0 eV. The optical energy gaps of the p-and n-layers were kept constant at 2.0 eV. The thickness of the i-layer was set at 500 Å. The thresholds of the voltage lie from about 7 V -17 V depending on the optical energy gap of the i-layer. The increase of the threshold voltages with increasing the optical energy gap of the i-layers is due to the increases of the height of the notch barriers at the p/i and i/n interfaces as well as the series resistance in the i-layer. The TFLEDs with the optical energy gaps of the i-layer = 2.6 eV and 3.0 eV emitted red color light and yellow color light, respectively.

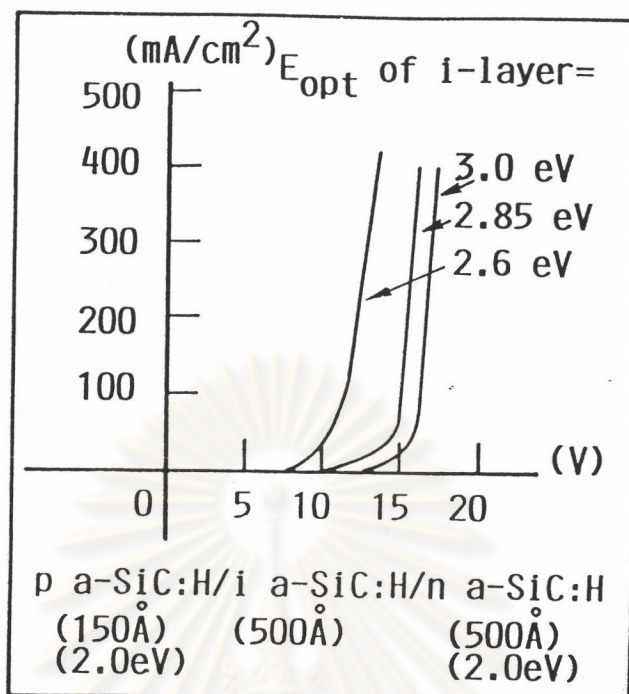


Figure 4.7 Room temperature I-V curves of a-SiC:H TFLEDs. The parameter is the optical energy gap of the i-layer i.e., 2.60, 2.85 and 3.0 eV, respectively.

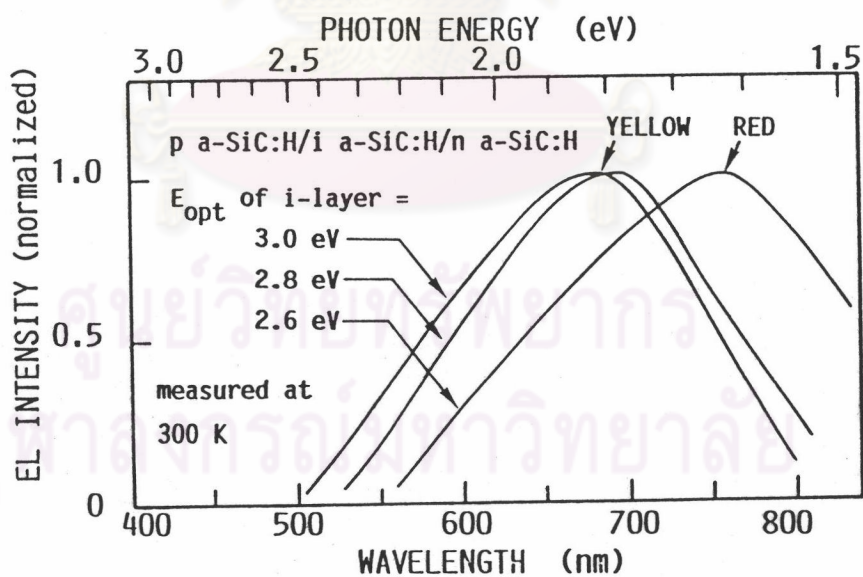


Figure 4.8 Room temperature EL spectra of a-SiC:H TFLEDs. The parameter is the optical energy gap of the i-layer i.e., 2.60, 2.85 and 3.0 eV, respectively.

4.6.2 Electroluminescent (EL) Spectra

A series of a-SiC:H TFLEDs consisting of the i-layers of various optical energy gaps have been fabricated. By changing the optical energy gap of the luminescent active i-layer from 2.60 eV to 3.0 eV, we have succeeded in fabricating red, orange and yellow color emitting TFLEDs.

Figure 4.8 shows the EL spectra measured at room temperature. The parameter is the optical energy gap of the i-layer 2.60 eV, 2.85 eV and 3.0 eV, respectively. The forward injection current for the measurement was 100 mA/cm². For the sample of the optical energy gap of i-layer = 2.60 eV, the EL spectrum peaks at 1.60 eV, with full width at half maximum (FWHM) = 0.4 - 0.5 eV (red emission). The 2.85 eV sample exhibits a broad band peaking around 1.75 eV with FWHM = 0.4 - 0.5 eV (orange emission). The 3.0 eV sample has their peaks around 1.85 eV with FWHM = 0.4 - 0.5 eV (yellow emission). The electroluminescence from these samples are bright enough to be observed in a bright room.

It is interesting to point out that all of the peak energies of the spectra lie in the photon energies lower than the corresponding optical energy gaps. This is because the radiative recombination takes place at the localized states down below the gap.

4.6.3 Relationship Between Brightness and Current Injection Density of a-SiC:H TFLED

Figure 4.9 shows the relationship between the brightness of the a-SiC:H TFLED and the injection current density. The parameter E_{opt} is the optical energy gap of the i-layer. The brightness increases as the injection current increases. The slope of the curve is close to unity, however the brightness seems to saturate at the high current density. The maximum brightness of about 1-2 cd/cm² is obtained in the yellow TFLED.

In this figure, it is interesting to mention that the brightness of the a-SiC:H TFLEDs increases as the optical energy gap of the i-layer increases. This implies that the number of the radiative recombination centers in the localized states seems to increase when the carbon content increases.

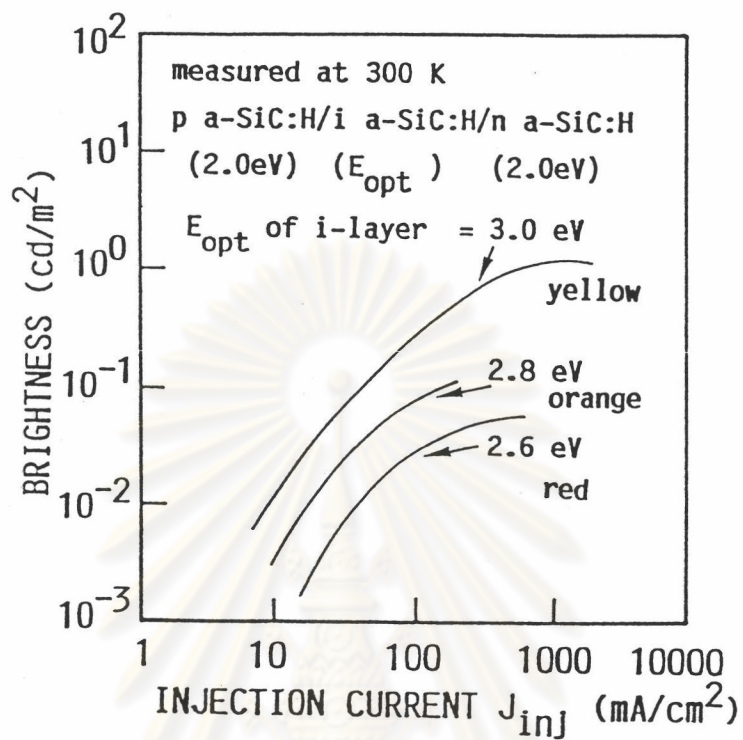


Figure 4.9 Relationship between the brightness of the a-SiC:H TFLED and the injection current density. The parameter E_{opt} is the optical energy gap of the i-layer.

ศูนย์วิทยทรัพยากร
 จุฬาลงกรณ์มหาวิทยาลัย

The result is consistent with the result of the measurement of the dependence of the localized states on the carbon contents [17]. Nonomura et al. reported that as the carbon contents in a-SiC:H increase the density of the localized tail states near the energy at which radiative recombination occurs increases. The tendency in Fig. 4.9 for the a-SiC:H TFLEDs is in the opposite direction of the case for the a-SiN:H TFLEDs as shown in chapter 3. The brightness of the a-SiN:H TFLED decreases as the optical energy gap of the i-a-SiN:H increases. It was interpreted as due to the increase in the barrier height for holes and electrons to tunnel as the optical energy gap of the i-a-SiN:H increases.

4.6.4 Dependence of EL Intensity on the Frequency-Modulation

Figure 4.10 shows the waveforms of the light output response to square-wave current pulse input for a yellow a-SiC:H TFLED. The frequency of the square-wave current pulse ranges from 500 Hz to 20 kHz. The duty cycle of the pulse current is 50 % and the modulation current amplitude was kept constant. It was found that the rise time and fall time of the waveform of the light output are several microseconds.

Figure 4.11 shows the dependence of the integral intensity of the light emission from the yellow a-SiC:H TFLED on the frequency of the pulse current. It is found that the intensity of the light is constant at the frequency below 100 kHz and starts to decrease at the frequency above 100 kHz. The cut-off frequency at which the intensity of light is 70% of the value at low frequency is about 500 kHz. This experiment implies that the a-SiC:H TFLED can respond fast enough to the pulse current input with the frequency up to 500 kHz. The characteristic is good enough to confirm that the a-SiC:H TFLED can be used in a pulse current scanning mode as a flat panel display.

4.7 Fabrications and Demonstrations of a-SiC:H TFLED Displays

It has been shown in the previous section that the a-SiC:H TFLED can emit various color of light and the emissions are bright enough to be observed in a bright room. The brightness of the a-SiC:H TFLED is relatively better than a-SiN:H

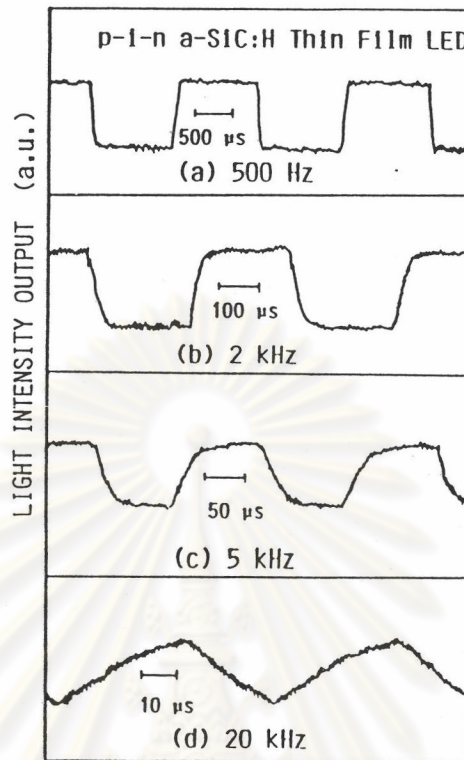


Figure 4.10 Waveforms of the light output response to a square-wave current pulse input for a yellow a-SiC:H TFLED.

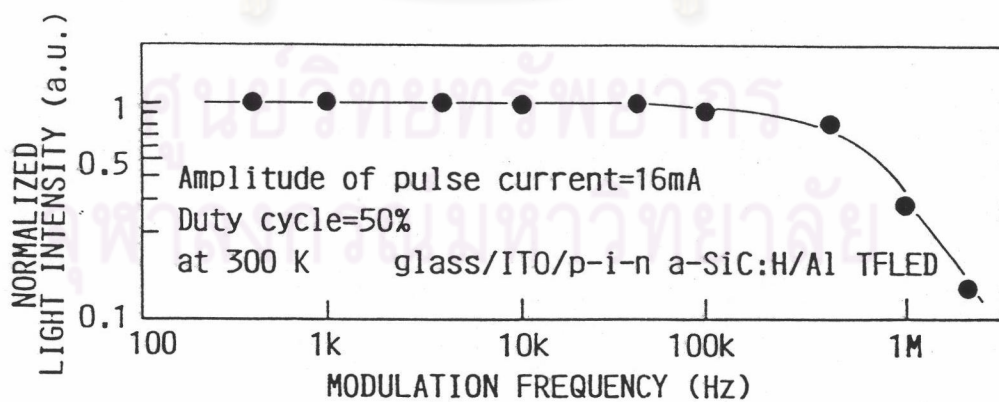


Figure 4.11 Dependence of the integral intensity of the light emission from the yellow a-SiC:H TFLED on the frequency of the pulse current.

TFLED. In this section, fabrication technologies and some demonstrations of a-SiC:H TFLED displays are briefly described.

A desired emitting pattern of the a-SiC:H TFLED display can be achieved by designing a pattern of either an ITO transparent front electrode or an Aluminium rear electrode. Figure 4.12 shows the photographs of the various masks used in a photolithography process for etching the ITO electrode.

Figure 4.13 shows the photographs of several actual a-SiC:H TFLED displays before emitting light. The ITO front electrodes were etched into desired patterns. The a-SiC:H and Al films were deposited onto the whole area of the substrate.

Figure 4.14 shows a photograph of an actual emission from a yellowish-orange a-SiC:H TFLED with a rectangular pattern and area of $3 \times 5 \text{ mm}^2$. The emitting pattern was determined by the Al rear electrode.

Figure 4.15 shows a photograph of a yellow color emission from an a-SiC:H TFLED. The emitting pattern is the symbol of "Telephone Organization of Thailand". The pattern was determined by the ITO electrode. The size of emission area is about $2 \times 2 \text{ cm}^2$.

Figure 4.16 shows a picture of a yellow color emission from an a-SiC:H TFLED. The emitting pattern is "Gear" which is the symbol of the Faculty of Engineering, Chulalongkorn University. The pattern was determined by the ITO electrode. The diameter of the emission area is 16 mm.

Figure 4.17 shows a photograph of a yellowish orange color emission from an a-SiC:H TFLED. The emitting pattern is "Cat". The pattern was determined by the ITO electrode. The height of the pattern is 16 mm.

Figure 4.18 shows a photograph of a yellowish orange color emission from an a-SiC:H TFLED. The emitting pattern is "MRS" which is the symbol of the Materials Research Society, U.S.A. The pattern was determined by the ITO electrode. The height of the pattern is 7 mm.

Figure 4.19 shows a photograph of a yellowish orange color emission from an a-SiC:H TFLED. The emitting pattern is "SSDM" which is the symbol of "Solid

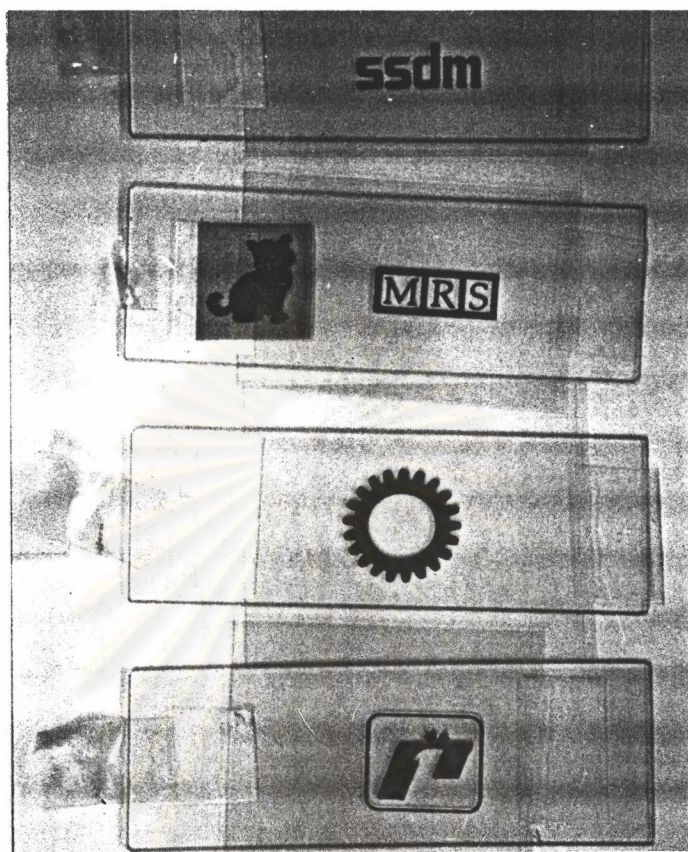


Figure 4.12 Photographs of various masks used in a photolithography process for etching an ITO electrode.

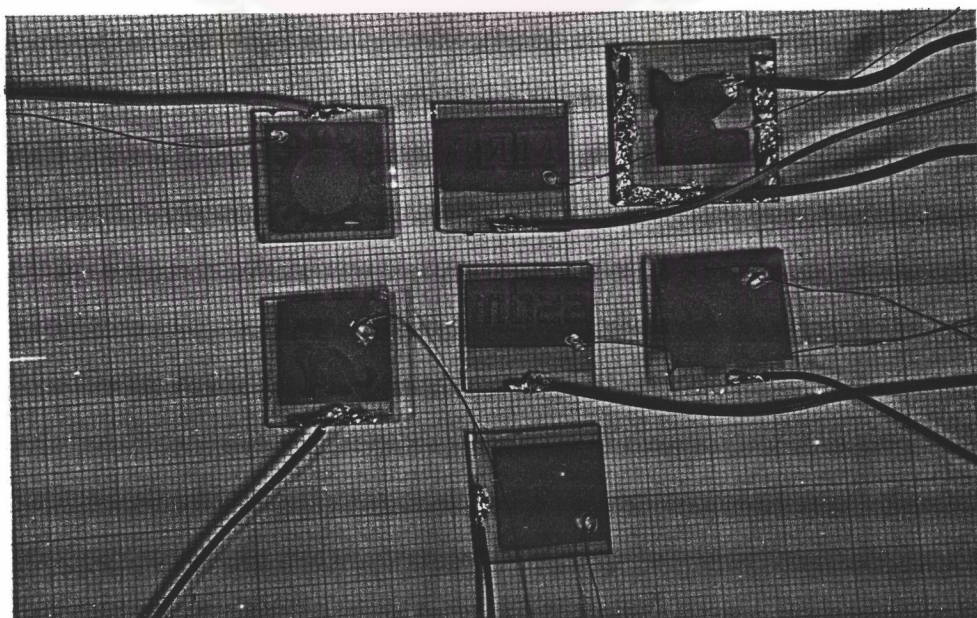


Figure 4.13 Photographs of several a-SiC:H TFLED displays fabricated in the work.

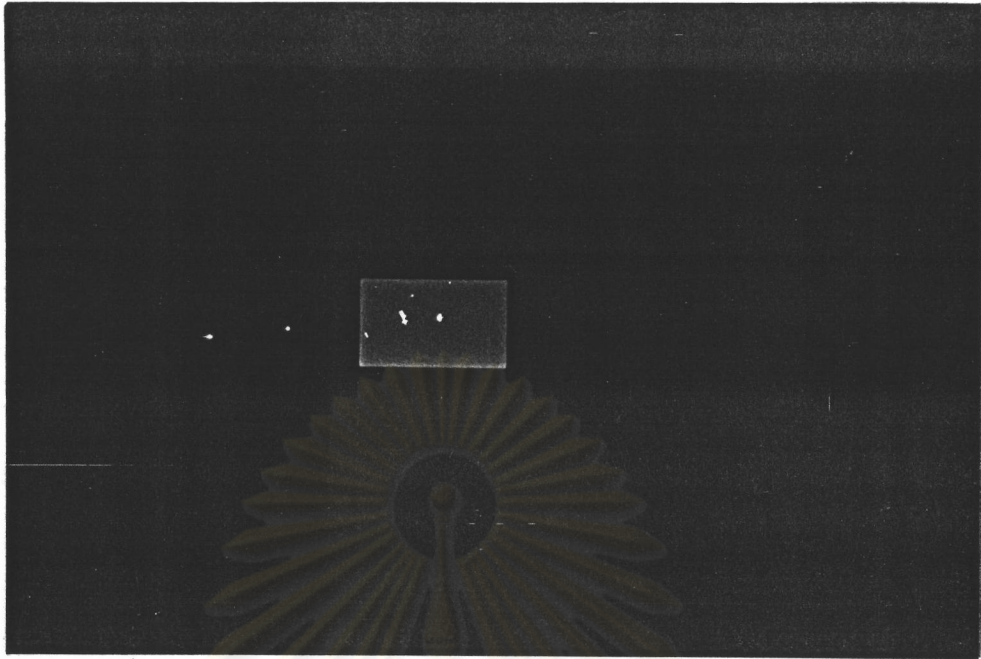


Figure 4.14 Photograph of an actual emission from a yellowish-orange a-SiC:H TFLED with a rectangular size of $3 \times 5 \text{ mm}^2$. The emitting pattern is determined by the Al rear electrode.

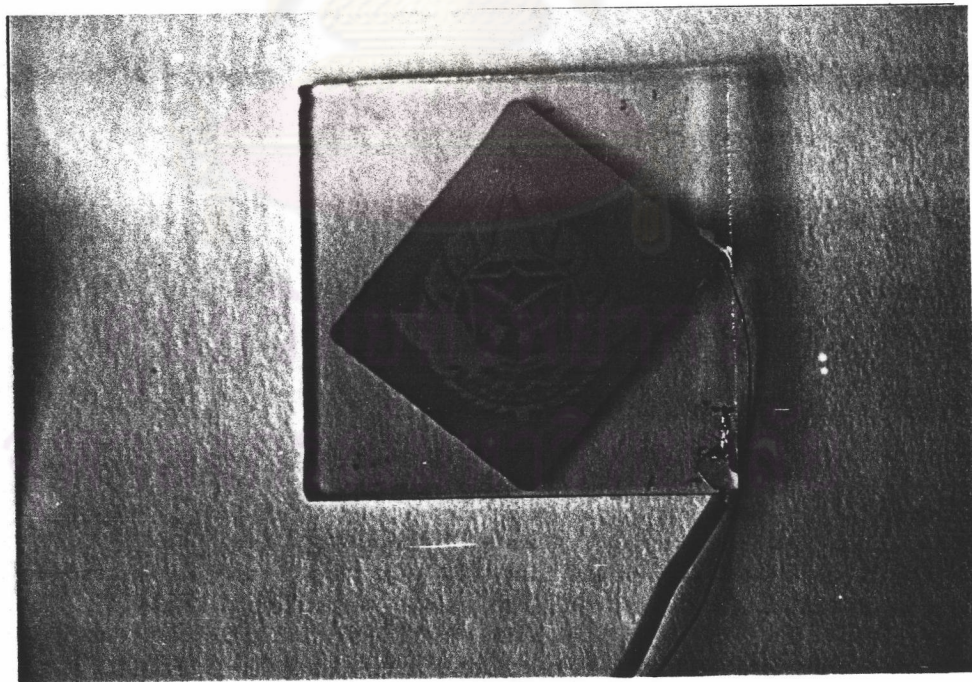


Figure 4.15 Photograph of a yellow color emission from an a-SiC:H TFLED. The emitting pattern is the symbol of the Telephone Organization of Thailand.

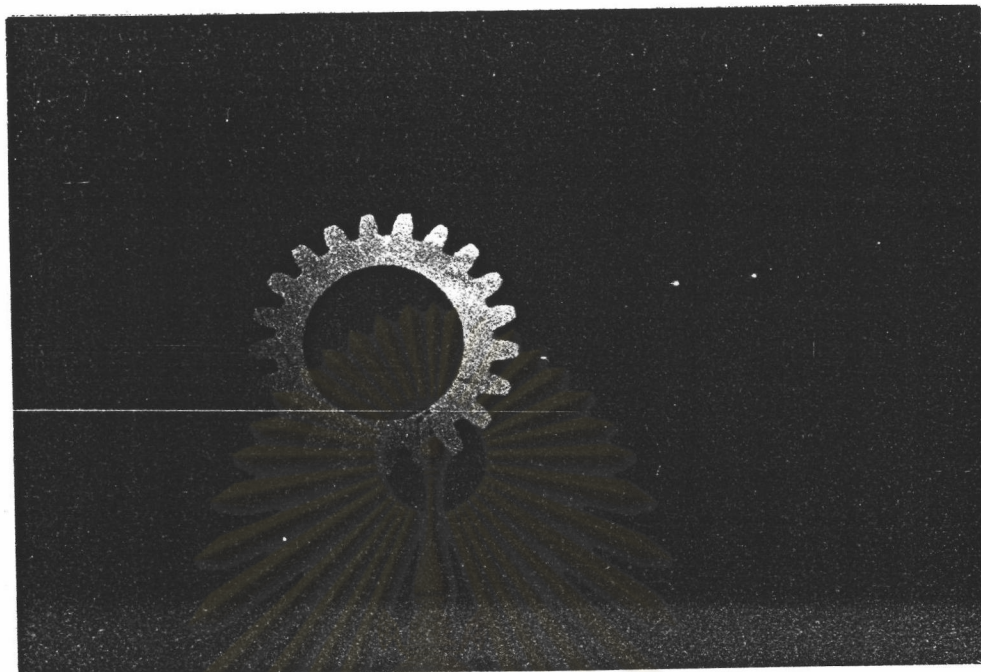


Figure 4.16 Photograph of a yellow color emission from an a-SiC:H TFLED. The emitting pattern is “Gear” which is the symbol of the Faculty of Engineering, Chulalongkorn University.



Figure 4.17 Photograph of a yellowish orange color emission from an a-SiC:H TFLED. The emitting pattern is “Cat”. The height of the pattern is 2 cm.

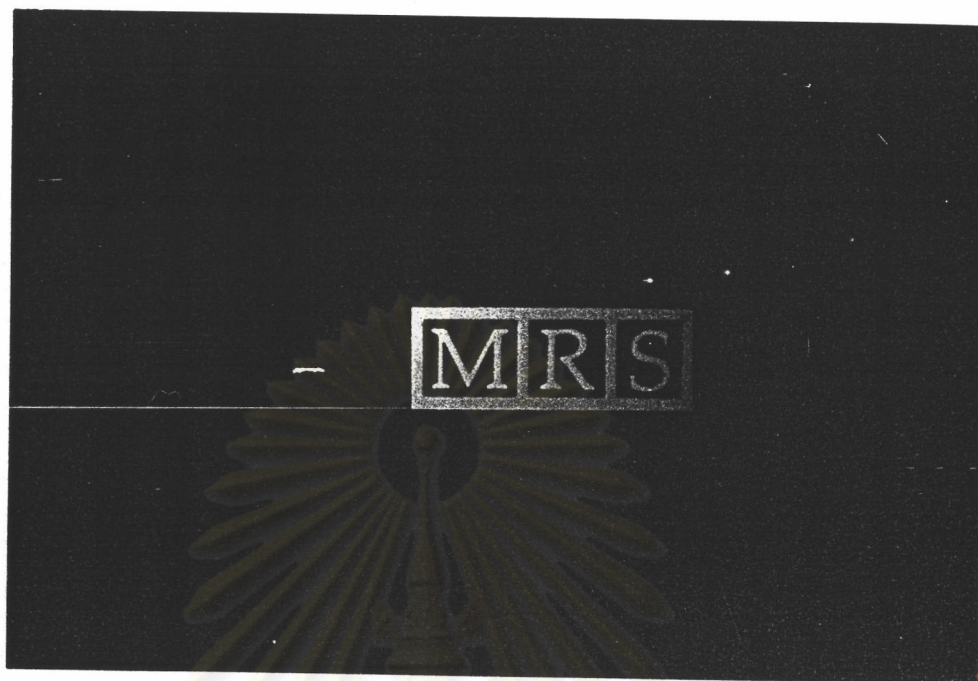


Figure 4.18 Photograph of a yellowish orange color emission from an a-SiC:H TFLED. The emitting pattern is “MRS” which is the symbol of the Materials Research Society, U.S.A..



Figure 4.19 Photograph of a yellowish orange color emission from an a-SiC:H TFLED. The emitting pattern is “SSDM” which is the symbol of “Solid State Devices and Materials Conference”.



Figure 4.20 Photograph of a yellowish orange color emission from an a-SiC:H TFLED. The emitting pattern is the symbol of “Premier Group of Company”.

ศูนย์วิทยทรัพยากร
จุฬาลงกรณ์มหาวิทยาลัย

State Devices and Materials Conference”. The pattern was determined by the ITO electrode. The height of the pattern is 4 mm.

Figure 4.20 shows a photograph of a yellowish orange color emission from an a-SiC:H TFLED. The emitting pattern is the symbol of “Premier Group of Company”. The pattern was determined by the ITO electrode. The height of the pattern including frame is 14 mm.

4.8 Summary

Hydrogenated amorphous silicon carbide (a-SiC:H) with wide optical energy gap from 1.8 eV to 3.1 eV was prepared by the glow discharge plasma CVD method. The visible photoluminescence can be observed in the a-SiC:H with the optical energy gap wider than about 2.3 eV.

A visible-light a-SiC:H p-i-n junction thin film LED (a-SiC:H TFLED) has been developed. The brightness of the a-SiC:H TFLED is 1-2 cd/m² which is bright enough to be observed in a bright room. The brightness of the a-SiC:H TFLED is better than that of the a-SiN:H TFLED (0.7-0.8 cd/m²) described in chapter 3. It has also been shown for the first time that the a-SiC:H TFLED can be operated by a pulse current mode with the modulation frequency as high as 500 kHz. This frequency is high enough to use the a-SiC:H TFLED in a scanning mode as a new type of flat panel display. The yellow and orange color a-SiC:H TFLED with various emitting patterns have been fabricated and demonstrated.

ศูนย์วิทยทรัพยากร
จุฬาลงกรณ์มหาวิทยาลัย

References

1. Anderson, D.A and Spear, W.E. Electrical and optical properties amorphous silicon carbide, silicon nitride and germanium carbide prepared by the glow discharge technique. Phil. Mag. 35 (January 1977) : 1-16.
2. Engemann, D., Fischer, R., and Knecht, J. Photoluminescence in the amorphous system $a\text{-Si}_x\text{C}_{1-x}$. Appl. Phys. Lett. 32 (September 1978) : 567-569.
3. Wieder, H., Cardona, M., and Guarnieri, C.R. Phys. Status Solidi. B 92 (1979) : 99.
4. Sussmann, R.S. and Ogden, R. Photoluminescence and optical properties of plasma deposited amorphous silicon alloy. Phil. Mag. B 44 (January 1981) : 137-158.
5. Kruangam, D. Amorphous and microcrystalline silicon-carbide alloy light emitting diodes. In J. Kanicki (ed.) , Physics and properties, in amorphous and microcrystalline semiconductor devices: optoelectronic devices, pp. 165-240. Artech House : Boston, London, 1991.
6. Tawada, Y., Okamoto, H., and Hamakawa, Y. Appl. Phys. Letts. 39 (1981): 237.
7. Morimoto, A., Miura, T., Kumeda, M., and Shimizu, T. Defects in hydrogenated amorphous silicon-carbon alloy films prepared by glow discharge decomposition and sputtering. J. Appl. Phys. 53 (1982) : 7299-7305.
8. Munekata, H., Murasato, S., and Kukimoto, H. White photoluminescence of amorphous silicon-carbon alloy prepared by glow-discharge decomposition of tetramethylsilane. Appl. Phys. Lett. 37 (September 1980) : 536-537.
9. Munekata, H., Shiozaki, A., and Kukimoto, H. Composition-dependent stokes shift to photoluminescence in amorphous SiC. J. Lumin. 24-25 (1981) : 43-46.
10. Kruangam, D., Deguchi, D., Toyama, T., Okamoto, H., and Hamakawa, Y. Carrier injection mechanism in an $a\text{-SiC:H}$ p-i-n junction thin film LED. IEEE Trans. Electron Devices. ED-35 (1988) : 957-965.

11. Engeman, D. and Fisher, R. Proc. 5th Int. Conf. Amorphous and Liquid Semiconductor (J. Stuke and W. Brenig, eds. 1974) : 947.
12. Street, R.A. Semiconductor and Semimetals. 21 B (1984) : 197.
13. Collins, R.W., Paesler, M.A., and Paul, W. The temperature dependence of photoluminescence in a-Si:H alloys. Sol. Stat. Commun. 34 (1980) : 833-836.
14. Shah, J., Pinczuk, A., Alexander, F.B., and Bagley, B.G. Excitation wavelength dependence of luminescence spectra of a-Si:H. Sol. Stat. Commun. 42 (1982) : 717-720.
15. Tsang, C and Street, R.A. Luminescence decay in glow-discharge deposited amorphous silicon. Phil. Mag. B 37 (1978) : 601-608.
16. Watanabe, I., Hata, Y., Morimoto, A., and Shimizu, T. Photoluminescence in glow discharge deposited amorphous SiC:H films. Jpn. J. Appl. Phys. 21 (1982) : L613-l616.
17. Boonkosum, W., DeLong, B., Kruangam, D., and Panyakeow, S. Novel visible amorphous silicon carbide thin film LED. The 1st International Symposium on Laser and Optoelectronics Technology and Applications (ISLOE). Singapore. (November 11-14, 1993) : 300-305.
18. Kruangam, D., Boonkosum, W., Ratwises, B., Panyakeow, S., and DeLong, B. Visible-light amorphous silicon alloys thin film light emitting diodes and its applications to optoelectronic functional devices. Proceeding of the 8th International School on Condensed Matter Physics (ISCMP) -Electronic, Optoelectronic and Magnetic Thin films- Varna. Bulgaria. (September 18-23, 1994) : 87-94.
19. Kruangam, D., Boonkosum, W., Ratwises, B., Sujaridchai, T., and Panyakeow, S. Fabrication of amorphous silicon alloy optical devices for new types of thin film optoelectronic integrated circuits. Proceedings of the 13th Australia Microelectronics Conference (MICRO'95), Adelaide Hilton, Adelaide South Australia, July 16-19 (1995) : 259-264.

20. Kruangam, D. and Boonkosum, W. Novel thin film light emitting diode display made of amorphous silicon based semiconductors. The 1994 Spring Meeting of Materials Research Society (MRS), Vol. 345 -Flat Panel Display Materials, San Francisco, U.S.A., (April 4-8 1994) : 305-310.
21. Nonomura, S., Sakata, S., Kamada, T., Kida, H., Kruangam, D., Okamoto, H., and Hamakawa, Y. Detailed studies of optical edge and below gap absorption in a-Si_{1-x}C_x:H system. J Non-Crys. Solid. 77&78 (1985) : 865-868.



ศูนย์วิทยทรัพยากร
จุฬาลงกรณ์มหาวิทยาลัย